Azimuthal signal variations in the engineering array of the Pierre Auger Observatory

K.S. Caballero-Mora*
Forschungszentrum Karlsruhe.

L. Nellen
Instituto de Ciencias Nucleares, UNAM,
e-mail: lukas@nucleares.unam.mx

J.F. Valdés-Galicia
Instituto de Geofísica, UNAM.

We study the azimuthal variation of the signal in selected tanks in the engineering array of the Pierre Auger Observatory. We fi a parametrization to the observed variations. We also note that the observation of the signal variations can be used to detect mistakes in the wireing from the PMTs to the control board.

Keywords: Extensive air showers; cosmic rays; Cherenkov detectors; observatories; detectores Cherenkov.

Estudiamos la variación azimutal de las señales detectadas en tanques seleccionados de la red de ingeniería del Observatorio Pierre Auger. Ajustamos una parametrización a las variaciones observadas. También notamos que es posible analizar las variaciones para detectar errores en el cableado entre los tubos fotomultiplicadores y la tarjeta controladora.

Descriptores: Chubascos atmosféricos; rayos cósmicos; detectores Cherenkov; observatorios.

PACS: 95.55.Vj; 96.50.sd; 96.50.S-; 29.40.Ka; 95.45.+i

1. Introduction

The Pierre Auger Observatory was conceived to measure the flux arrival direction distribution and mass composition of cosmic rays to the very highest energies with high statistical significanc over the whole sky. To achieve this aim, the Observatory will have instruments located at two sites, one in the Southern and another in the Northern Hemisphere. Arising largely from the expectation of spectral features in the decade above 10^{19} eV, the astrophysical interest in this energy range is well known. According to theoretical predictions, the energy spectrum should steepen sharply above about 6×10^{19} eV due to the interaction of primary cosmic rays with the microwave background radiation [1]. These predictions, commonly known as the Greisen-Zatsepin-Kuzmin (GZK) cut-off, are still the subject of considerable controversy. It is clear that there are cosmic rays with energies well beyond 10^{20} eV; major issues are the flu of these events and the accurate measurement of the spectral shape. It is known that the spectrum of cosmic rays extends to at least 3×10^{20} eV [2–4].

Above 10^{20} eV, the rate of events is about $1 \, \text{km}^{-2} \, \text{sr}^{-1} \, \text{century}^{-1}$; therefore vast areas must be monitored to collect a large statistical sample. The Pierre Auger Observatory has been planned as a pair of arrays, each measuring $3000 \, \text{km}^2$. The design calls for 1600 water-Cherenkov detectors, arranged on a triangular grid, with the sides of the triangles measuring $1.5 \, \text{km}$, overlooked by four optical stations, each containing six telescopes, designed to detect air-fluorescenc light (Fig. 1). The water-tanks respond to the particle component (mainly muons, electrons and positrons) and the fluorescenc cameras measure the emission from atmospheric nitrogen that is excited by the charged particles of the shower as they traverse the atmosphere. Both techniques, already used for many years to study extensive air showers (EAS) [3–5], are brought together in a 'hybrid' detector to observe showers simultaneously with different techniques. The array of water-tanks is known as the surface detector (SD) while the optical stations form the fluorescenc detector (FD).

The surface array will have the following properties:

- 100% duty cycle.
- A fi ed, well-define aperture that is independent of energy above 10^{19} eV.
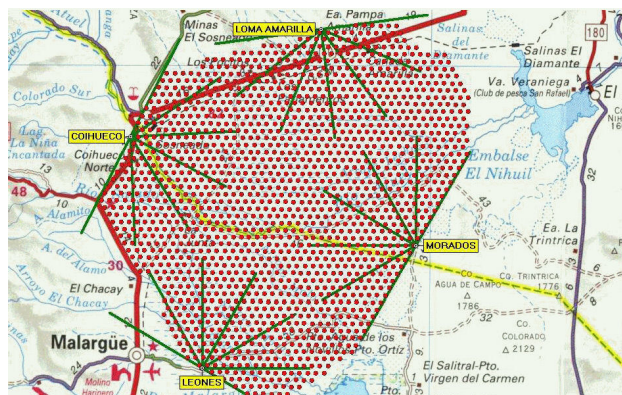
FIGURE 1. The layout of the Pierre Auger Observatory.

- Uniform coverage in right ascension on a daily basis.
- A response that is largely independent of weather conditions.
- The quality of the data for each event improves with energy.
- Sensitivity to showers arriving at large zenith angles.
- *In situ* calibration of the detectors by cosmic ray muons.
- Measurement of the time structure of the arriving signals, which is sensitive to the mass of the primary particles.

The fluorescenc detectors can be operated during clear nights with little moonlight and have the following characteristics:

- Every event above 10^{19} eV is registered by at least one fluorescenc detector: 60% of these events will be recorded by two or more fluorescenc detectors. Essentially every trans-GZK event will be a stereo event. Multiple station coverage improves the energy resolution.

- A coincidence of a single detector of the surface array with a single fluorescenc telescope constrains the shower geometry as precisely as a stereo fluorescenc detector.

- The longitudinal development profil is measured directly.

- The fluorescenc detectors provide a more direct measure of the shower energy. The small, unseen, fraction of the total energy carried by neutrinos and muons that is predicted depends somewhat on the mass of the primary particle as well as on the hadronic interaction model.

The design for the Observatory was developed through a series of workshops, starting in Paris in 1992, and culminating in a six-month study at Fermi National Accelerator Laboratory in 1995. The design is well suited to resolve the discrepancies at the high energy end of the cosmic ray spectrum that have been reported by the AGASA surface array [3] and the HiRes fluorescenc detector [4], since it is the firs and only large-scale experiment to combine both techniques.

At present, the Southern Hemisphere Observatory of the planned pair is being built in Argentina. The firs phase of the project was the construction and operation of a prototype system, known as the engineering array (EA). This made it possible to test the integration of all of the sub-systems that will be used in the full instrument and to verify their correct operation under fiel conditions. The EA comprised 32 fully instrumented water tanks and 2 FD telescopes at one site.

In addition, the engineering array gave us the opportunity to gain better knowledge of the detailed functioning of the different components of the detector. In this paper we

study the azimuthal signal variations in the photo multipliers (PMTs) of the water tanks that constitute the elementary stations of the SD due to light that is not fully diffused light. The aim is to produce a proper conversion of the light received by the PMTs when the Cherenkov light emitted by the particles entering the water tank hits one of these light detectors directly.

In what follows we shall firs describe the SD components and functioning [6]. The basic unit of measurement (Vertical Equivalent Muon, VEM) is define and the sources of uncertainty involved in the light detection and conversion into an electrical digital signal are described in Sec. 2. In Sec. 3 we shall explain how we selected the tanks and events of the EA used in this study. Section 4 is dedicated to the presentation of our results; there we propose an algorithm to correct for the azimuthal variations when all three PMTs are operative and to have a realistic estimate of the full signal of a Cherenkov tank when one of the PMTs is broken. Conclusions are briefl stated in Sec. 5. A study similar to the one presented here has been done focusing on horizontal air showers [7–9].

2. The surface detector of the observatory

A particle with a velocity greater than the speed of light in a medium will produce Cherenkov light. The cosmic ray secondary particles (mainly muons, electrons and positrons) generated in the atmosphere by a high energy cosmic ray become superluminic in water. This Cherenkov light they emit is captured by three special PMTs of 20cm diameter, located inside a water tank.

The basic unit of the SD is a water tank that is cylindrical in shape with a $12,000$ liter capacity. It has a cross section of $10 \, \text{m}^2$ (diameter of $3.6 \, \text{m}$) and a depth of $1.2 \, \text{m}$. The 1600 tanks of the SD array will be separated by a distance of $1.5 \, \text{km}$ in a triangular grid as shown in Fig. 1. Every tank is equipped with three PMTs $20 \, \text{cm}$ in diameter, and the PMTs are located above the water of the tank inside light protecting boxes. The tank has to support the stresses brought by the solar panels on top of them in strong winds. Three hatches provide access to each of the PMTs; one hatch being wider to allow for the connection of the PMTs to the electronics enclosure. The tanks are solar-powered and communicate via a wireless network with the central data acquisition system. This design has been implemented by building rotationally molded tanks with a special resin to produce long-life products with good molding properties, a necessity to assure a smooth interior.

To guarantee the opacity of the tank, the resin used is hot-compounded with 1% of carbon black pigment. However, to reduce the ecological impact of black tanks in the sandy, yellowish landscape of the Pampa Amarilla, and the effect of heating on sunny days, the tank is rotomolded in two layers, the external one being compounded with a beige pigment. The tank interior surface is covered with a liner, and a

cylindrical Polyolefi bag is used to contain the detector volume inside the tank. The bag is mechanically supported by the tank, and must provide a 20 year seal for the water, high reflect vity of Cherenkov light and act as a secondary seal against extraneous light sources. In addition, it must protect the water from contamination and inhibit bacteriological activities. At a distance of 1.2 m from the centre of the top of the tank, at three symmetric locations in the top of the liner, polyethylene dome windows are fitte for the installation of the PMTs.

The tanks are fille with ultra pure water so that its transparency will be maintained over the 20-year lifetime of the experiment. Extreme care is taken to prevent water from becoming contaminated during the transport or tank-fillin procedures.

These characteristics assure that the tanks are completely opaque to external light, have an effective reflecto -diffuser of light as internal cover and biological activity is inhibited in the stored water.

Muons are abundant particles in the cosmic ray secondary flu forming a well-understood and uniform background. The signal produced by muons inside the tank is proportional to their path length. This fact is used as a basis to have a unit of measurement of the signal produced in the tanks by any particle. The unit is called the Vertical Equivalent Muon (VEM) and it is the average signal produced by muons crossing the water vertically along the axis of the station. To obtain a one VEM signal, a "muon telescope" is constructed with two scintillators located above and below the Cherenkov tank and use their coincidences as triggers for the three PMTs inside. In this manner the charge distribution over a PMT signal over any time interval of measurement will have a peak at the signal corresponding to one VEM [6, 10]. The VEM provides a practical way of normalising signals from different detectors and expressing the total signal of every station in a shower in terms of an equivalent reference. Stations are calibrated with respect to this absolute value of the VEM with an overall precision of 5%.

Measurements obtained within the SD stations have several uncertainty sources that may be classifie into two main groups:

1. Sampling fluctuation due to the uncertainty in the knowledge of shower development:

   (a) the energy of the primary,
   (b) the place of the firs interaction (this can not be measured),
   (c) the zenith angle,
   (d) the distance of the tank to the shower core and
   (e) the lateral distribution. This gives the changing particle distribution with the distance to the core.

2. Uncertainties caused by the detector itself such as:

   (a) Photostatistics. The Cherenkov signal expansion in the three PMTs give Poisson fluctuation in the number of photoelectrons released in the PMTs.

(b) Systematic fluctuations Due to detector instability and electronic noise.

(c) Azimuthal effect. Water and the lined walls of the tank are not perfect diffusers. Thus the number of Cherenkov photons arriving at each PMT will vary depending on the angle of incidence of the particles. If this angle coincides with that of one of the three PMTs, light will reach it directly, thus creating an asymmetry amongst the three. Similarly, light that bounced only once or twice off the detector walls still has a correlation with the original direction and will contribute to asymmetries. The total signal will depend mostly on the privileged PMT.

It is this last effect that is the motivation for the research presented here. A proper knowledge of the azimuthal signal variations is crucial for a precise determination of the tank response. This knowledge will have consequences in determining the lateral distribution function that provides the localization of the shower core and an estimate of the primary energy as well [11]. The PMT positions and privileged directions are illustrated in Fig. 2. As already pointed out, the PMTs in the tank are separated at an angle of 120°. As indicated in Fig. 2, the privileged direction for PMT1 is -150°, for PMT2 is 90°, and -30° for PMT3. Practical reasons motivate the location of the PMTs in the tank cover. The solar panel is oriented facing north to track the sun and the battery is placed on the south side to avoid exposure to direct sunlight. The PMTs are 120 cm away from the tank axis and they are numbered 1, 2 and 3 clockwise from the solar panel.
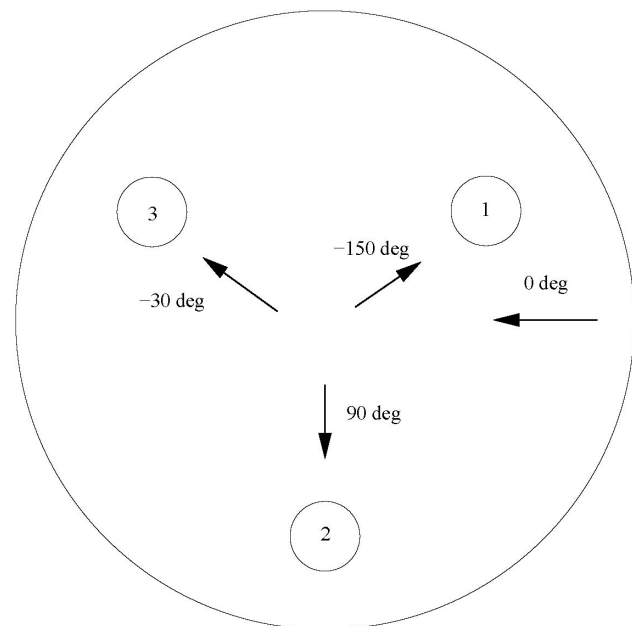
FIGURE 2. PMT Positions and preferred directions for signal asymmetries.

TABLE I. Characteristics of the selected stations.

Name	Number	PMT type	Comment
Ursula	36	Hamatsu	All PMTs OK
Susana	44	ETL	All PMTs OK
Tamara	46	Hamatsu	All PMTs OK
Flavia	63	ETL	All PMTs OK
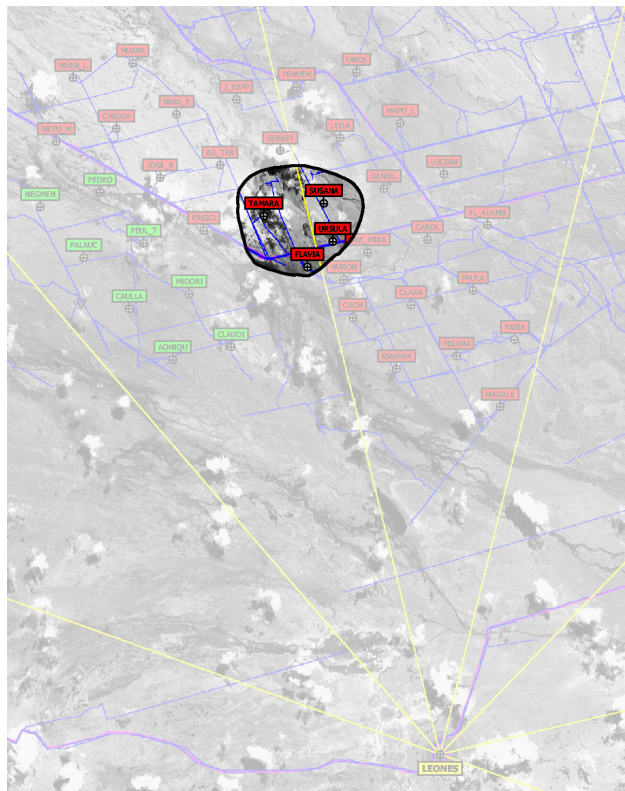
FIGURE 3. Tank positions in the Engineering Array. The tanks used in this study are marked.

3. Event analysis

The basic aim of this research is to study azimuthal variations of the signals detected in the SD stations of the Auger Observatory and to produce a means of correcting for these effects in the total signal of the tank. Another objective is to fin a way to reconstruct the signal of a station when one of the PMTs is not working.

We have done the analysis based on the signals of one tank where the three PMTs are functional. We discarded the signal of one of them to reconstruct the results of the whole tank for a selection of events. The procedure was repeated for each of the three PMTs. Results of the reconstructed signal differ from the original one by 5% at the most. The method of correction was implemented in a second tank where the three PMTs were also operative and of the same type as the original. This time, the differences of reconstructed and original signals were the same within 10%. This means that our

procedure for signal reconstruction was validated for all the Auger SD stations with that PMT brand type.

As a fina test for the method, we repeated the procedure for a third tank with PMTs of a different brand. The relevant differences were 7% in this case. Thus our method is also independent of the type of PMTs used.

3.1. Tank and event selection

We based our selection of tanks from the EA on the operation of the array between 20 august 2002 and 15 April 2003, as this is the time range when we had a maximum number of tanks in operation. Once the time interval was fi ed, we tried to select tanks that were in the middle of the EA surface array to guarantee that the events used were completely contained. We also tried to select tanks within the densest part of the array where there is more likely to be a higher number of tanks triggered in the events to be considered. To have good statistics we also required that the selected stations register at least 1000 events within the period considered. The tanks chosen were 36 (Ursula), 44 (Susana), 46 (Tamara) and 63 (Flavia), and are shown in Fig. 3, their main characteristics are contained in Table I.

We considered events where

1. At least four stations besides the tank to be studied were triggered.

2. The triggered stations should be within the firs or second neighbours of the relevant station. This guarantees that the selected events are of the highest energies and that they are not the consequence of random coincidences.

3. To check that the event reconstruction was not erroneous determination in the angle, we imposed the restriction that the sum of the squares of the direction cosines $u = \sin\theta\cos\phi$ and $v = \sin\theta\sin\phi$ of the reconstructed direction should be less than or equal to one. Random signals in some tanks or other problems with an event can cause this physical condition to be violated.

4. Another restriction to prevent random coincidences was to consider only events for which the core of the shower was within $10\,\mathrm{km}$ of the selected station.

5. We only accept events that could be reconstructed successfully, as measured by the quality of the fit to determine the incoming direction, the core position, and energy. Signal uncertainties are not known for the EA. As a consequence, the χ^2 function was not properly normalized and we had to use ad-hoc cuts. We obtained a clean sample of events by imposing $\chi^2 < 1000$ for the initial fi (preliminary direction) and $\chi^2 < 2 \times (\text{number of stations}) - 3$ for the fina fi (direction, core position, energy).

The Carmen-Miranda pair (a couple of stations separated by only 10 m) was considered as only one station for event selection.

The Fortran Analysis Software Tool was used to access the event data. We modifie the user subroutine to match our selection criteria and also to extract from the original fil only the data to be used in our study.

To have an explicit check of our selection criteria against an independently produced routine, the Event Display program produced by the Central Data Acquisition System was used. This program shows a reconstructed lateral distribution function, the incidence zenith and azimuth angles, the distance from the core and the primary energy reconstruction in a graphical form.

4. Results

With the stated selection criteria we were left with 1202 events for the Ursula station, 656 for Susana, 348 for Tamara (here we had to consider events with core distances beyond 10 km) and 838 for Flavia. Ursula was used as the tank to develop our analysis method since it had the highest number of events. Tamara was the station selected to test the correction method developed as the equipment was the same as that of Ursula. Susana had too few events registered and was fi nally not used in the analysis. We verifie the universality of our method with the signals of Flavia, which had different equipment.

Figure 4 presents the azimuthal variations for PMT3 of Ursula. The signals from the three PMTs were normalised using the average signal of all the PMTs per event. In the plots, the maxima correspond to the phases derived from the location of each PMT as expected: -150° for PMT1, 90° for PMT2 and 150° (or -30°) for PMT3. The most obvious analytical approximation of the variation of the signal fraction P_i in PMTi as a function of the azimuth angle ϕ is of the form [8]:

$$P_i = A_i \sin(\phi - k_i) + b_i \tag{1}$$

where A_i is the amplitude of the variation in the ith PMT, k_i is the corresponding phase, and b_i is the baseline factor. Since the data are normalised, the b_i should be one for perfectly gain-matched PMTs. Therefore $b_i - 1$ is an estimate of the gain mismatch amongst the three PMTs, and its variance is a measure of the noise in the PMTs. The results of the proposed fi for the three PMTs of Ursula is shown in Table II. Note that the values of b_i are consistent with one and in any case deviations are less than one percent.

TABLE II. Results of fittin Eq. (1) to data from Ursula.

PMT	Amplitude (A)	Phase (k)	b
1	0.066 ± 0.03	120	1.007 ± 0.02
2	0.075 ± 0.03	0	0.983 ± 0.02
3	0.070 ± 0.03	-120	1.005 ± 0.02
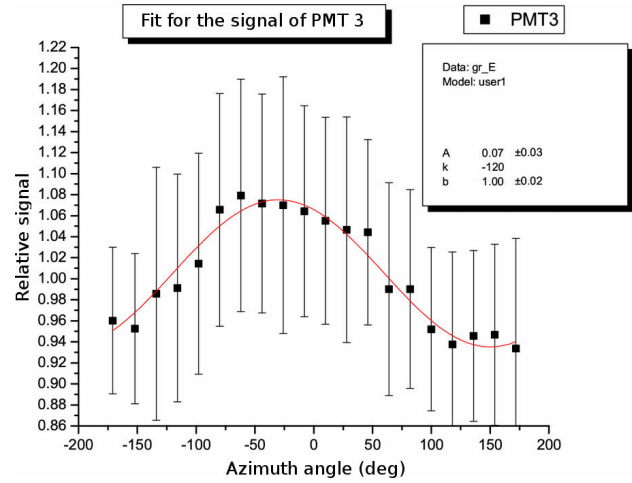
FIGURE 4. Fit of angular dependence of relative signal strength for PMT 3 of Ursula.

To make the fi of the data to the analytical form of Eq. (1), data were binned in 20 intervals of 18 degrees each. For each bin the data were averaged. Results of the fi for PMT3 of Ursula are presented in Fig. 4, where the squares represent the median values and the error bars are the full width at half maximum of the distributions in each bin. The data follow the fi reasonably well as the correlation coeffi cient is close to one and the χ^2 test gives a very small number.

As the proportion of the Cherenkov light cone hitting the PMT depends on the zenith angle of arrival, the parameters of the fi may vary accordingly. Therefore we decided to divide the data according to the zenith angle of arrival of the shower. We have chosen to divide the sky into three regions with the same solid angle namely from 0 to 41°, 42 to 60° and 61 to 90°. Equation (1) was fitte to the data of every PMT for the three different zenith angle intervals. Results are presented in Table III.

Again the baseline of the signal is consistent with one in all cases. The amplitude of the signal grows in all three PMTs as the zenith angle increases, indicating the growth of the fraction of the Cherenkov cone that is seen by the PMTs.

To take into account this zenith dependence of the amplitude, we can generalise Eq. (1) as:

$$P_i = A_i(\theta) \sin(\phi - k_i) + b_i. \tag{2}$$

A linear fi was used to get $A(\theta) = m * \theta + s$. Results are shown in Table IV.

Intercepts are consistent with zero and the three slopes are the same within statistical error. We may therefore make a unique fi representing all three PMTs of the Ursula tank with the average points of the three intervals and fi the intercept at zero. Thus the slope for Ursula is $m = 0.00161 \pm 0.00017$.

Once we have parameterised the signal shape and amplitude for the Ursula station, the next stage is to test its ability to reconstruct the full signal assuming that one of the PMTs is broken or malfunctioning. We have done this in two different ways and compared the results with those produced by

TABLE III. Results of fittin Eq. (2) to data from Ursula in individual zenith-angle bands.

	PMT 1		PMT 2		PMT 3	
Zenith	A	b	A	b	A	b
0–41	0.039 ± 0.025	1.00 ± 0.02	0.048 ± 0.025	0.98 ± 0.02	0.042 ± 0.025	1.01 ± 0.02
41–60	0.089 ± 0.023	1.00 ± 0.02	0.091 ± 0.022	0.99 ± 0.02	0.090 ± 0.006	1.00 ± 0.004
60–90	0.112 ± 0.016	1.02 ± 0.01	0.134 ± 0.014	0.98 ± 0.01	0.112 ± 0.011	1.00 ± 0.01

TABLE IV. Fit to get $A(\theta) = m * \theta + s$ for Eq. (2).

PMT	slope (m)	intercept (s)
1	0.0015 ± 0.0004	0.0006 ± 0.02
2	0.0018 ± 0.0003	-0.0014 ± 0.02
3	0.0015 ± 0.0004	0.0085 ± 0.02
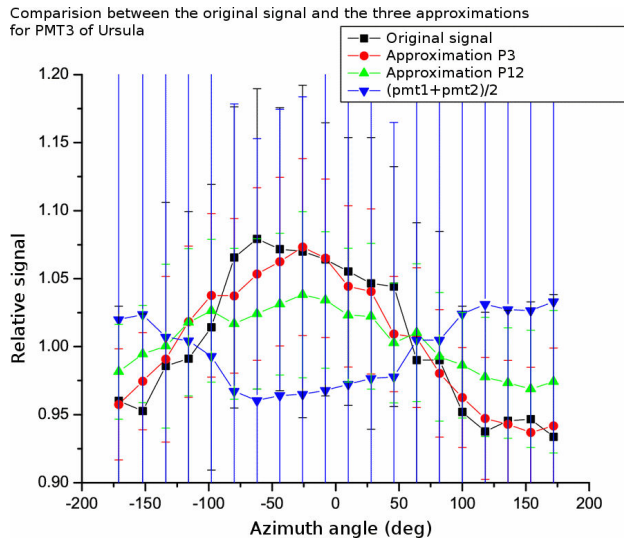
FIGURE 5. Comparison of the three approximation schemes to replace a missing signal for PMT3 of Ursula.
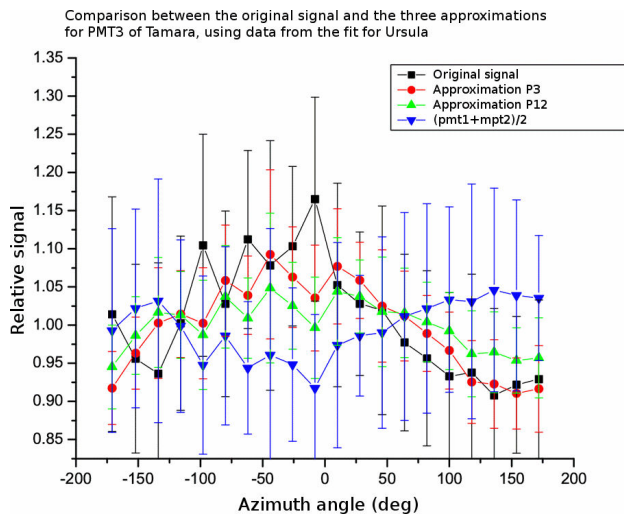
FIGURE 6. Comparison of the three approximation schemes to replace a missing signal for PMT 3 of Tamara, using the parameters from Ursula.

a simple substitution where no azimuthal effects are taken into account.

The total tank signal is:

$$\bar{V} = \frac{V_1 + V_2 + V_3}{3}. \tag{3}$$

If V_3 is missing then it can be approximated simply by

$$V_3 = \frac{V_1 + V_2}{2}. \tag{4}$$

This approximation does not take into account the azimuthal effect just presented in this work. We will call this the firs approximation.

Instead, we use Eq. (1) with Eq. (3) to take into account the PMT phases. We have to solve the resulting equation

$$V_3 = \bar{V}\left(1 + A_3(\theta)\sin(\phi - k_3)\right)$$
$$= \frac{V_1 + V_2 + V_3}{3}\left(1 + A_3(\theta)\sin(\phi - k_3)\right) \tag{5}$$

for V_3. We call the result the P_i approximation.

Alternatively, one can write the analogue of Eq. (5) for PMT1

$$V_1 = \bar{V}\left(1 + A_1(\theta)\sin(\phi - k_1)\right) \tag{6}$$

and similarly for PMT2. Both equations can be solved for V_3. We call the average of the two solutions the P_{ij} approximation.

In the ideal case, where the A_i and b_i are the same for all three PMTs, the two approximations P_i and P_{ij} coincide. Since this is not the case here (see, *e.g.*, Table III), we get different answers, depending on how we estimate the signal of a missing PMT.

We compare the results of using each of the three approximations to the real value of V_3 in Fig. 5. From the figur we see that the best approximation is P_3 (method P_i). The differences of P_i from the original signal is not more than 5%. Of the three methods, P_i is the only one where the azimuthal effect is clearly recognisable.

Up to this point we have shown that we are able to reproduce the total signal of an SD station when one of the PMTs is missing or malfunctioning. We now apply the method to see if it may be used in any other tank with the same type of PMT. In Fig. 6 we present the results of the approximation of the signal corresponding to PMT3 of the station Tamara using the parameters of the fi in Ursula. Again it can be easily

TABLE V. Result of fit to tank *Flavia*, which uses different PMTs

PMT	Amplitude (A)	Phase (k)	b
1	0.096 ± 0.04	-120	1.02 ± 0.03
2	0.094 ± 0.04	0	0.996 ± 0.03
3	0.083 ± 0.04	120	0.981 ± 0.03
a) Amplitudes, phases, and baselines			

Zenith	PMT 1	PMT 2	PMT 3
$0 - 41$	0.062 ± 0.03	0.056 ± 0.03	0.054 ± 0.03
$42 - 60$	0.107 ± 0.03	0.091 ± 0.03	0.087 ± 0.03
$61 - 90$	0.222 ± 0.04	0.249 ± 0.03	0.194 ± 0.04
b) Amplitudes in different zenith ranges			

PMT	Slope (m)	Intercept (b)
1	0.0028 ± 0.0007	-0.015 ± 0.034
2	0.003 ± 0.0006	-0.024 ± 0.028
3	0.0023 ± 0.0007	-0.012 ± 0.039
c) Amplitude fi as function of zenith		
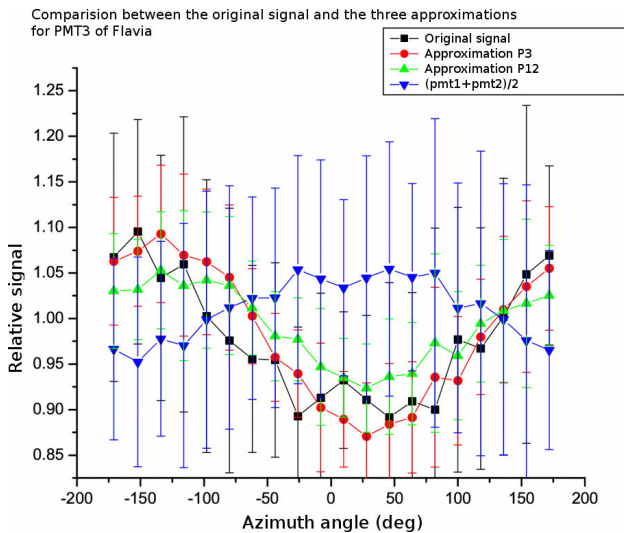
FIGURE 7. Comparison of the three approximation schemes to replace a missing signal for PMT 3 of Flavia.

appreciated that the best results are those of the P_i approximation. Differences between our approximation and the real signal are not more than 10%, thus showing that the param-

eters obtained for one tank may be used in the correction of any other tank with identical equipment.

The fina test that we carried out was to apply it to the signals of Flavia, which had a different type of PMTs installed. Results of the parameter calculations done with the signals of Flavia are presented in Table V. Although the numbers are not the same, the main conclusions arising from the calculations done for the Ursula parameters also apply to Flavia: the three PMTs are properly gain-matched, there is a growth of signal amplitude with zenith angle, the amplitude dependence with zenith angle is the same for all three PMTs (slope $= 0.00247 \pm 0.00039$), and the amplitude fi is consistent with symmetry around the vertical.

Comparison between the three different approximations with the real signal is shown in Fig. 7. Again the best approximation corresponds to the adjustment of the signal using P_i. From the figur it can be seen that the maximum of the signal is around -30° and not at -150° as it should in order to correspond to the PMT1 (see Fig. 2). This means that the cables for PMT1 and PMT3 are swapped in Flavia. Therefore an additional use of the method developed here is to fin stations where the cables have been wrongly tagged. Only a few hundred events are necessary to identify these misconnections with the PMT signal dependence on azimuthal angle.

5. Summary and conclusions

We have conducted a study to better understand the response of the SD of the Southern Auger Observatory. We selected four tanks of the SD installed for the EA of the Observatory to analyse the signals produced by showers with different arrival zenith and azimuthal angles in order to identify azimuthal signal variations in the PMTs. We can summarise the results found in this research as:

1. An azimuthal effect is identifiabl in the SD stations.

2. The gain balance of the three PMTs for a station can be cross-checked with the method developed here.

3. The full signal from a tank can be recovered in a faithful manner depending on the azimuthal and zenith arrival angle when a PMT is broken or malfunctioning.

4. Correct identificatio of the PMTs can be checked with our method.

∗ Previously at: Instituto de Ciencias Nucleares, UNAM.

1. K. Greisen, *Phys. Rep. Lett.* **16** (1966) 748; G.T. Zatsepin and V.A. Kuz'min, *JTEP Lett* **4** (1966) 78.

2. M. Nagano and A.A. Watson, *Rev. Mod. Phys.* **72** (2000) 689.

3. M. Teshima *et al.*, *Nucl. Instr. Methods A* **247** (1986) 399.

4. R.M. Baltrusaitis *et al.*, *Nucl. Instr. Methods A* **240** (1985) 410;

P. Sokolsky, *Proceedings of Workshop on Observing Giant Cosmic Ray Air Showers from* $> 10^{20}$ *eV Particles from Space*, AIP Conf Proc No. 433, edited by J.F. Krizmanic, J.F. Ormes, and R.E. Streitmatter, NY 1998, p. 65.

5. J. Linsley, L. Scarsi, and B. Rossi, *Phys. Rev. Lett.* **6** (1961) 458; J. Linsley, *Phys. Rev. Lett.* **10** (1963) 146; G. Cunningham *et al.*, in *Catalogue of Highest Energy Cosmic Ray*, edited by M.

Wada (World Data Center of Cosmic Rays, Institute of Physical and Chemical Research, Itabashi, Tokyo) Vol. 1 (1980) 61; M.A. Lawrence, R.J.O. Reid, and A.A. Watson, *J. Phys. G* **17** (1991) 733; B.N. Afanasiev *et al.*, in *Proceedings of the Tokyo Workshop on Techniques for the Study of the Extremely High Energy Cosmic Rays*, edited by M. Nagano (Institute for Cosmic Ray Research, University of Tokyo, Tokyo, Japan, 1993) p. 35

6. The Pierre Auger Collaboration, *Nucl. Instr. Methods A* **523** (2004) 50.

7. A. López-Agüera, V.M. Olmos-Gilbaja, and G. Rodríguez Fernández, "Direct light in inclined showers", Auger technical note GAP-2003-112.

8. A. López-Agüera, V.M. Olmos-Gilbaja, and G. Rodríguez-Fernández, "Direct Light Impact parameter dependence in a Cherenkov water tank", Auger technical note GAP-2004-026.

9. A. López-Agüera, V.M. Olmos-Gilbaja, and G. Rodríguez-Fernández, "Removing Direct Light From HAS", Auger technical note GAP-2004-061.

10. F. Alcaráz *et al.*, *Nucl. Instr. Methods* **420** (1999) 39.

11. Markus Roth (for the Pierre Auger Collaboration), "The Lateral Distribution Function of Shower Signals in the Surface Detector of the Pierre Auger Observatory", proceedings of the XXIIXth Cosmic Ray Conference, Tsukuba, Japan, 2003, p. 333.